water

MDPI

Article

Analysis of the Occurrence Conditions and Formation Mechanism of Mineral Water in the Southern Region of Yaoquan Mountain, Wudalianchi

Chang Li [1,2], Xubin Shan [3,*], Chuansheng Li [4,5,*], Shuren Hao [6,7], Bin Cheng [6], Chuanlei Lu [1,2], Jian Zhao [1,2], Xu Wang [1,2] and Ziliang Su [1,2]

1 Harbin Center for Integrated Natural Resources Survey, China Geological Survey (CGS), Harbin 150086, China; 13845114316@163.com (C.L.); 15045064006@163.com (J.Z.); wangxuheb@163.com (X.W.)
2 Observation and Research Station of Earth Critical Zone in Black Soil, Harbin, Ministry of Natural Resources, Harbin 150086, China
3 Institute of Ecological Geology Survey and Research of Heilongjiang Province, Harbin 150030, China
4 Hebei Key Laboratory of Close-to-Nature Restoration Technology of Wetlands, School of Eco-Environment, Hebei University, Baoding 071002, China
5 Shandong GEO-Surveying & Mapping Institute, Ji'nan 250012, China
6 School of Civil and Architectural Engineering, East China University of Technology, Nanchang 330013, China; dr_haosr@163.com (S.H.); 15170392871@163.com (B.C.)
7 Nanchang Key Laboratory of Hydrogeology and High Quality Groundwater Resources Exploitation and Utilization, Nanchang 330095, China
* Correspondence: wudisxb@163.com (X.S.); lichuansheng1983@163.com (C.L.)

Abstract: Because of its unique geographical properties, the Yaoquanshan area of Wudalianchi City, Heilongjiang Province, contains rich mineral water resources. We have carried out much research on the mineral water in the Yaoquanshan area of Wudalianchi City, which has also been supplemented by of previous studies. In this paper, through a controlled audio geoelectromagnetic method, geological drilling, groundwater level monitoring and water quality analysis, the structure, regional geology, hydrogeology and water geochemistry, as well as the characteristics of the distribution of metasilicate mineral water and natural soda water, the formation mechanism and the recharge, runoff and excretion of groundwater in the study area, are discussed. The results can provide a theoretical basis for the exploitation and utilization of mineral water resources in the southern region of the Wudalianchi Pharmaceutical Spring Mountain.

Keywords: mineral water; hydrogeology; distribution characteristics; formation mechanism

check for updates

Citation: Li, C.; Shan, X.; Li, C.; Hao, S.; Cheng, B.; Lu, C.; Zhao, J.; Wang, X.; Su, Z. Analysis of the Occurrence Conditions and Formation Mechanism of Mineral Water in the Southern Region of Yaoquan Mountain, Wudalianchi. *Water* **2024**, *16*, 3130. https://doi.org/10.3390/w16213130

Academic Editors: Xudong Zhang, Shuang Tian, Shengyi Cong, Xudong Zhou and Yiding Bao

Received: 6 October 2024
Revised: 23 October 2024
Accepted: 29 October 2024
Published: 1 November 2024

Copyright: © 2024 by the authors. Licensee MDPI, Basel, Switzerland. This article is an open access article distributed under the terms and conditions of the Creative Commons Attribution (CC BY) license (https://creativecommons.org/licenses/by/4.0/).

1. Introduction

Natural mineral water is a unique liquid mineral formed by dissolving beneficial mineral components and trace elements in water during the circulation process under specific geological conditions [1]. Such bodies of water are not only rich in composition, but are also widely appreciated for their special health effects [2]. The formation of mineral water is related to many factors related to the surface and underground environments, particularly geological structures, rock type, groundwater movement and its interaction with the outside world [3]. In recent years, the examination of natural mineral water has gained momentum as public interest in health and wellness continues to rise. As consumers become more health-conscious, the demand for high-quality natural products with proven health benefits has increased. This trend has intensified research into the chemical properties and health implications of mineral water resources, positioning them as pivotal resources in both wellness tourism and alternative medicine.

Wudalianchi City, situated in the heart of the Keluo–Wudalianchi–Erjiashan volcanic activity zone, serves as both an active volcanic eruption site and a significant tectonic

fault zone [4,5]. The geological characteristics of this area contribute to the optimal conditions for mineral water formation that can be found there. The presence of volcanic rocks and Mesozoic pyroclastic rocks not only establishes favorable geomorphology for the enrichment and migration of mineral water but also enhances the dissolution and concentration of minerals and trace elements in the groundwater [6]. Consequently, the mineral water in the Wudalianchi area has garnered attention from both domestic and international researchers [7,8].

Recent advancements in science and technology have positioned the mineral water of Wudalianchi as a significant research focus. Multiple studies indicate that the mineral water in this region exhibits significant health benefits due to its distinct chemical composition, which includes metasilicic acid, lithium, strontium and various types of soda water [9–11]. The implications of these prevalent forms of mineral water for human health are increasingly being recognized. Furthermore, the potential applications of rarer mineral types, such as bicarbonate, carbonate, and radioactive radon, in health-related fields underscore the necessity for continued research in this area [12,13].

Wudalianchi sits within an ancient volcanic region characterized by complex and diverse geological structures. The residual volcanic and pyroclastic rocks from past eruptions yield a rich supply of minerals for mineral water production [14,15]. In the groundwater circulation process, the dissolution and concentration of beneficial minerals directly influence the characteristics of the resultant mineral water. These mineral constituents encompass, but are not limited to, magnesium (Mg), lithium (Li), strontium (Sr), bicarbonate and silicates, each possessing significant health-promoting functions [16,17]. For instance, metasilicic mineral water is acclaimed for its benefits to skin health due to its high silicate content, while lithium–strontium mineral water has demonstrated positive effects on mood and mental wellness thanks to its unique combination of trace elements [18]. The alkaline properties of soda water effectively neutralize acidic conditions in the body [18,19], promoting overall health. Additionally, bicarbonate, carbonate and radioactive radon mineral waters are traditionally utilized for their unique chemical compositions and energetic characteristics [20].

The Wudalianchi National Nature Reserve offers a wealth of mineral water resources, characterized by an exceptionally pure quality, complex compositions and an abundance of trace elements that are beneficial to human health [21]. According to established classification criteria, the mineral water from this locality can be categorized into ordinary and rare types. Research into ordinary mineral water is relatively well-developed, but further investigation is warranted for rare types, particularly bicarbonate and radioactive radon mineral water [22]. This research is critical not only for providing a reliable scientific basis for the health industry in the region but also in guiding relevant policy making and industrial development [23]. In terms of its practical applications, Wudalianchi's mineral water meets the daily drinking needs of local residents and attracts substantial tourism, enhancing the local economy and health sector [24]. This dynamic creates new opportunities for economic growth and promotes sustainable resource utilization [25].

This study aims to investigate the types, distribution and formation mechanisms of mineral water located in the southern region of Wudalianchi Yaoquan Mountain. To achieve this objective, the research will employ a combination of geological surveys, chemical composition analyses, and hydrogeological modeling. By integrating field data with laboratory analysis findings, the study seeks to comprehensively understand the occurrence conditions and genetic mechanisms of mineral water in this area. Through an in-depth examination of mineral waters, this research will provide critical data support for ongoing scientific inquiry and establish a theoretical framework for the rational utilization and sustainable development of mineral water resources.

2. Overview of the Study Area

2.1. Location of Study Area

Wudalianchi City is located in the northern portion of Heilongjiang Province, to the south of the Heihe region. It borders Nenjiang County to the northwest, and is adjacent to Bei'an and Kedong Counties to the southeast and southwest, respectively. To the west, it is bordered by Keshan and Nehe counties. The city is administratively under the jurisdiction of Heihe City. Spanning 142 km from east to west and 104 km from north to south, Wudalianchi City covers a total area of 8844 square kilometers. The study area used for this study is situated in the northwest of Wudalianchi City, under the administration of the Wudalianchi Tuanjie Town and the Wudalianchi Scenic Area Nature Reserve Management Committee. The region is easily accessible, with the Nev Highway traversing the entire study area from east to west. A location map of the study area can be found in Figure 1.

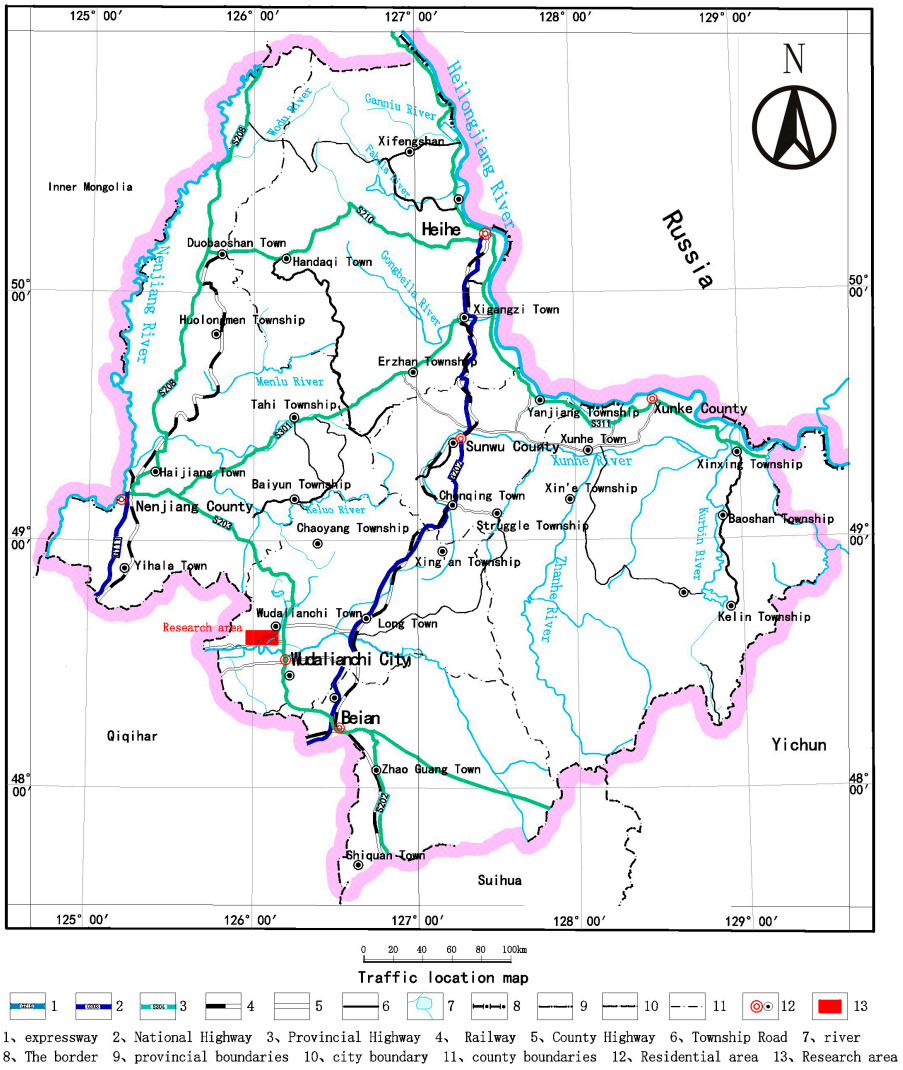


Figure 1. Map of the location of the study area.

2.2. Topography and Landforms

The study area is situated within a hilly high plain, bordering the Xiaoxing'an Mountains and the Songnen Plain. The highest elevation in this area reaches 600 m, while the lowest elevation is 248 m. Overall, the terrain trends are characterized by relatively high elevations in the eastern, northern and western parts, while the central and southern regions exhibit lower elevations.

The landforms in the study area can primarily be categorized into volcanic landforms and fluvial landforms based on their genetic types. A detailed breakdown of the landform types, units and morphologies present in the area is provided in Table 1.

Table 1. Landform description table.

Genetic Type	Morphological Unit	Description of Landform Morphology
Volcanic landform I	Undulating lava platform I_1	It is distributed around the shield-shaped platform. The table top has valleys formed by the action of flowing water, so the table top undulates. The elevation is 250–330 m, the ground slope is 24°, and it inclines towards the valley and the edge of the platform. It is covered with yellow silty clay intercalated with lava blocks, and below it is lava. Micro-landforms include massive lava piles (stone ponds) and recumbent stones.
Denudation and accumulation landform II	Hilly high plain II	It is located in the northwest of the area. The ground elevation is 290–370 m, with a relative height of 30–40 m. It is in the form of gentle slopes on undulating ridges. It is mainly composed of mudstone, sandstone, and argillaceous sandstone of the Nenjiang Formation (K1n) of the Cretaceous System. The surface is covered by residual-slope deposits.
Fluvial landform III	Terrace III_1	It is distributed on both banks of the Nehe River and belongs to the first and second terraces formed by river alluviation. The width of the first terrace is generally about 0.5–1.5 m. Most of its front edges have no obvious steep banks, and the back edges are 8–10 m higher than the floodplain. The ground elevation of the second terrace is 250–290 m. The width is generally 1–3 km. The front edges of most terraces form steep banks about 10 m high. The terraces belong to the Upper Pleistocene (Q3) of the Quaternary System and have a binary structure, consisting of silty clay on the upper part and a gravel layer on the lower part.
	Floodplain III_2	It is distributed in the south of the protected area and in the gullies in the area, formed by fluvial erosion and accumulation. The high floodplain is about 1–4 km wide, relatively flat, 2–3 m higher than the riverbed. There are many remaining oxbow lakes and puddles and swamps have developed. It has a binary structure and is composed of clay on the upper part and gravel on the lower part. The low floodplain is generally several meters to nearly a kilometer wide. The surface is undulating, overgrown with weeds or the gravel layer is exposed. The floodplain belongs to the Holocene (Q4) of the Quaternary System. Micro-landforms include gullies. "U"-shaped valleys have developed. Distributed on both sides of the hills and in the river valleys, mainly including gullies and wide valleys formed by downward cutting of flowing water and lateral erosion of rivers. The length of the gullies is relatively short, mostly within 2 km, and dozens to more than one hundred meters wide. Most of them are in the shape of a trumpet with a narrow upper part and a wide lower part. The bottom of the wide valley is flat and open, and there are many remaining ancient river channels, oxbow lakes, etc. The sedimentary layer in the valley is relatively thin, generally within 10 m. The valley slopes are mostly gentle slopes, mostly steep on the north slope and gentle on the south slope, showing an asymmetrical shape. Mostly slope–proluvial clay and gravels from the Holocene (Q4) of the Quaternary System are deposited.

2.3. Geological Structure

The Wudalianchi area is located in the Songnen interrupt (depression) zone of the XiaoXinganling–Songnen block in the Xinganling–Inner Mongolia geosynclinal fold area. About 30 km to the northeast is Sunwu Graben, and 20 km to the southwest is the Nemur River fault. The northeast-trending fault is the main structure, which is an inherited fault and was still active until the Quaternary period. Due to the control of the fault and the intrusion of magma, granite uplift and depression structures were formed, as shown in Figure 2.

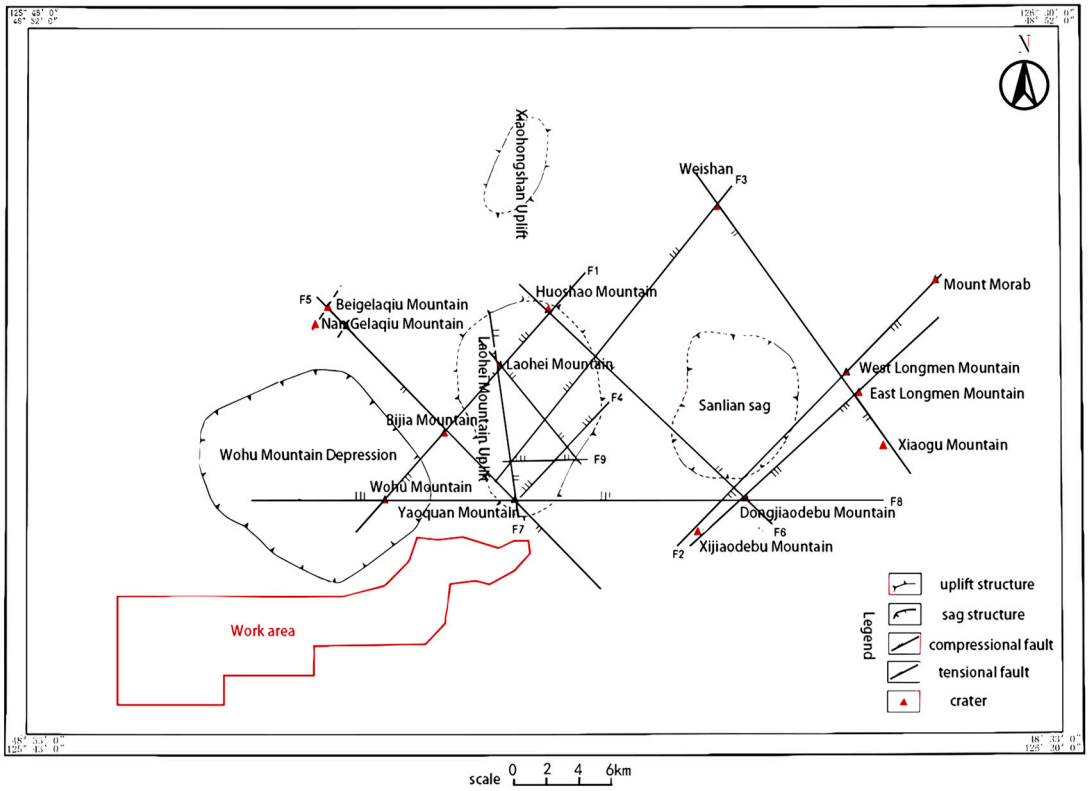


Figure 2. Regional structural outline.

(1) Fault structure

The fault structure developed in Wudalianchi area, and the fault in the direction of 45° NE is the main trunk fault. The 30–40° NW faults are also relatively well developed, and there are also north–south and near east–west faults nearby, both of which are smaller in scale. F1, F3 and F4 have an influence on the study area.

(2) Uplift and depression structures

Uplift structure: including the Yaoquanshan uplift in the middle and the Xiaohongshan uplift in the north, the axial direction is 10° northeast, the core is composed of Yanshanian granite, which is partially exposed at the surface, and the periphery is Triassic granite, mostly covered with thin Cretaceous rock layers.

Sag structure: located on both sides of the Yaoquanshan uplift, namely Sanlian sag and Wuhushan sag, the axial direction of the sag is nearly east–west, consistent with the direction of the east–west compressive and torsional fault of Yaoquanshan-Dongjiaodebu Mountain. The basement is Cambrian metamorphic rock with deep burial, and the Cretaceous deposits in the depression are thicker, about 300 m.

2.4. Geological Stratigraphy

Combined with data obtained from geophysical exploration and hydrogeological drilling, the exposed strata, from oldest to youngest, primarily consist of the Cretaceous Nenjiang Formation, the Lower–Middle Pleistocene Huangshan Formation, the Lower Pleistocene Weishan Basalt, the Upper Pleistocene Guxiangtun Formation and the Harbin Formation. The basic characteristics of these strata are summarized as follows:

(1) Cretaceous (K2n)

Cretaceous Nenjiang Formation (K2n): This formation is distributed throughout the area, with its thickness gradually increasing from northeast to southwest. The lithology is characterized by gray-green to gray-yellow fine sandstone and siltstone, interspersed with variegated mudstone and silty mudstone. Locally, interbedded sandstone and mudstone

are present. Thin layers of argillaceous glutenite can be found at both the top and bottom. The formation exhibits horizontal and cross bedding, contains minor amounts of charcoal debris, and has pyrite nodules or lenses, as well as a small number of plant fossils. The buried depth of the exposed Cretaceous roof ranges from 20.98 to 37.21 m, while the buried depth of the Cretaceous floor in the basalt platform area ranges from 79.65 to 204.13 m. Exploration wells in the high plain area did not penetrate the Cretaceous Nenjiang Formation. It is overlaid by the Lower–Middle Pleistocene Huangshan Formation and the Middle Pleistocene Weishan Basalt.

(2) Quaternary (QP)

Lower-Middle Pleistocene Huangshan Formation (Qp2h): This formation is distributed across the entire area, with a general thickness of less than 10 m. In the basalt platform area, it is buried beneath the basalt. The lithology mainly consists of yellow-brown silty clay and gravel; the silty clay is yellow, relatively fine-grained, slightly silty and exhibits a strong plasticity, with yellow rusty-brown spots or bands. The gravel is gray-yellow in color and primarily composed of acidic lava, displaying a poor roundness. The sand fraction contains feldspar and quartz. The buried depth of the exposed roof of the exploration wells ranges from 9.62 to 24.04 m, while the buried depth of the floor ranges from 14.36 to 27.32 m, showing an uneven thickness. This formation underlies the Cretaceous mudstone.

Middle Pleistocene Weishan Basalt (βQp2w): The lithology is primarily composed of pumice gravel, volcanic bombs, cinders, welded breccia conglomerate and basalt. This formation serves as the main target layer for metasilicic acid mineral water, which is distributed across the basalt platform. The buried depth of the exposed roof ranges from 7.00 to 29.45 m, while the buried depth of the floor ranges from 15.05 to 37.21 m, with thicknesses varying between 5.65 and 29.87 m. The thickness of this formation gradually decreases from northeast to southwest.

Upper Pleistocene Harbin Formation (Qp3h): This formation is widely distributed and primarily consists of two types of sedimentary materials: yellow-brown silty clay (resulting from alluvial-proluvial processes) and locally deposited lacustrine sedimentary silty clay. The former is predominantly found on undulating platforms, while the latter primarily occurs on the second terrace. The thickness of these sedimentary types on the surface varies from 3 to 10 m and from 5 to 14 m, respectively.

Upper Pleistocene Guxiangtun Formation (Qp3g): This formation is discontinuously distributed along both banks of the Nenhe River in the southern part of the study area, forming the residual first terrace of the river valley. The lithology mainly comprises gravel and silty clay with silt, with a thickness of approximately 11.5 m.

3. Research Methods

3.1. Controlled Source Audio-Frequency Magnetotellurics (CSAMT)

The CSAMT technique adopts the section measurement method. There are 4 CSAMT survey lines, with a total length of 7 km and 90 physical points, and the point distances are 50 m and 200 m, as shown in Figure 3. Through the processing and inversion interpretation of CSAMT data, the formation units and fault structure distribution through the section were obtained in this controllable source audio magnetotellurism sounding study. Data preprocessing and 2-D inversion of the CSAMT data for this section are carried out, and the resistivity models of each section are obtained. Combined with the geological, hydrological and geophysical characteristics of the survey area, the geological inference and interpretation of the resistivity model are carried out.

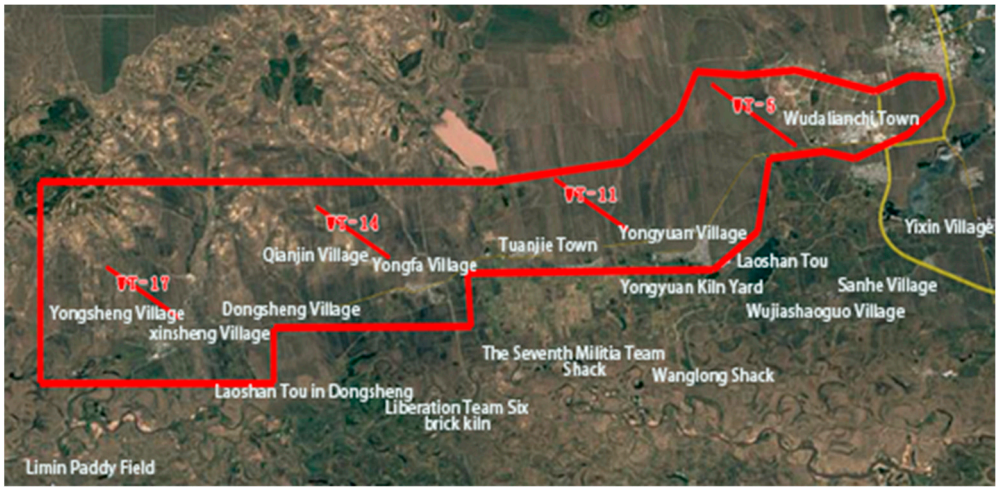


Figure 3. Relative position map of controlled audio magnetotelluric exploration lines.

3.2. Hydrogeological Survey

The survey route was perpendicular to the landform units, with each survey point located using handheld GPS devices. The positions of the survey points were marked on field maps, and the survey route was delineated. Simplified water level observation equipment was used to measure the depth of underground water levels at the hydrogeological survey points. A measuring tape was utilized to measure the height of the wellhead, well diameter and other features; the materials in the well casing were also recorded on-site. Local residents were consulted regarding the lithology and thickness of the groundwater aquifers, as well as the sensory characteristics of groundwater quality. Surveys and sampling of the wells and groundwater were conducted. We collected 21 sets of groundwater mineral water quality samples for detailed analysis. The testing methods employed included colorimetry, ion chromatography and atomic absorption spectroscopy. The analysis encompassed physical properties (such as color, taste and turbidity) as well as a range of standard chemical indicators (including HCO_3^-, CO_3^{2-}, Cl^-, F^-, Br^-, I^-, K^+, Na^+, Ca^{2+}, Mg^{2+}, TFe, Al^{3+}, Cd^{2+}, Pb^{2+}, Zn^{2+}, Hg^+, soluble SiO_2, $HsiO_3^-$, pH, mineralization, hardness, strontium, and metasilicic acid). Geological and geomorphological survey points were situated along geomorphological boundaries and within typical geological landform sites within the work area to verify the existing geomorphological and geological boundaries.

3.3. Groundwater Dynamic Monitoring

To further clarify the recharge mechanism of mineral water within the study area, an artificial monitoring approach was adopted to conduct groundwater dynamic monitoring over a period of one hydrological year for six exploration wells in the research area. The monitoring frequency was set to once every 10 days, totaling 272 monitoring sessions. The distribution of the monitoring wells is illustrated in the accompanying figure, with the following identifiers: QZK1, QZK2, QZK3, QZK4, SZK1, SZK2 and SZK3, as shown in Figure 4. Specifically, the dynamic monitoring periods for exploration wells QZK1, QZK2, QZK3, QZK4 and SZK1 were from 30 September 2021 to 30 October 2022; for SZK2, it was from 20 April 2022 to 10 April 2022; and for SZK3, it was from 10 August 2022 to 30 July 2023. All dynamic monitoring data collected are complete and valid, with the observational data being authentic and accurate, thereby achieving the intended research objectives.

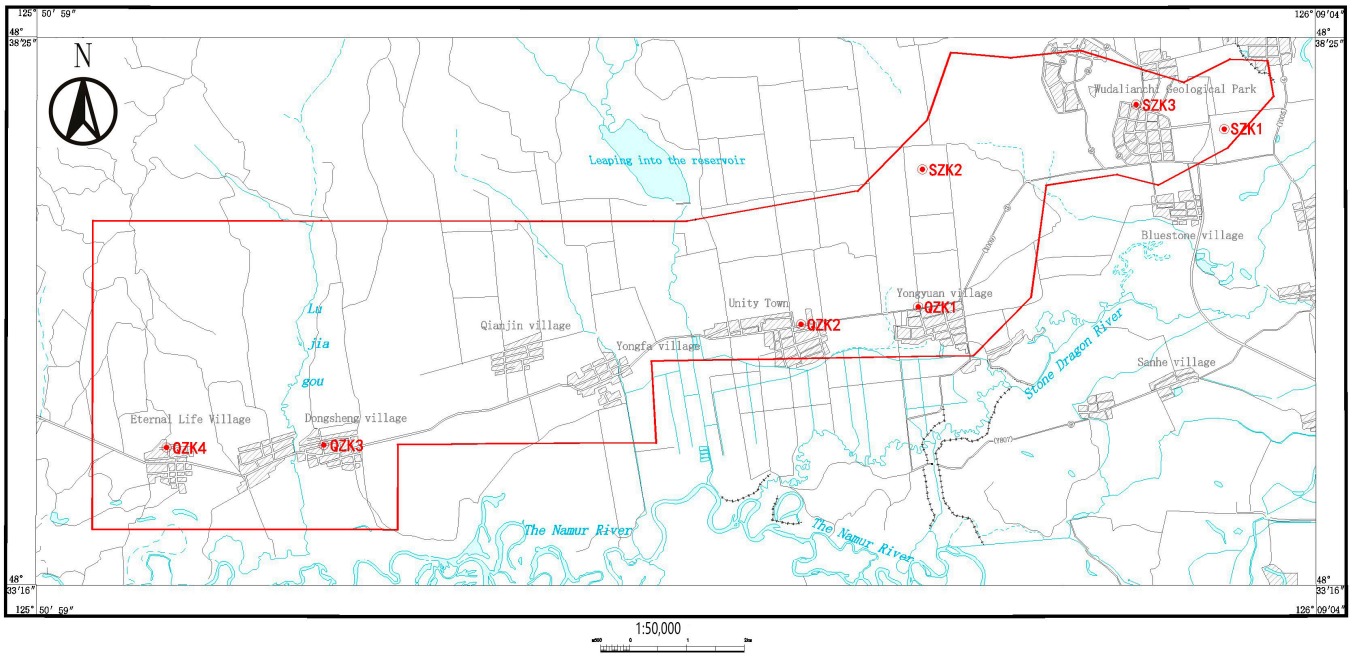


Figure 4. Distribution of groundwater monitoring Wells.

4. Results

4.1. Results of Controlled Source Audio-Frequency Magnetotelluric Depth Sounding

The geophysical survey employed controlled source audio-frequency magnetotellurics (CSAMT) to preliminarily identify the lithology, thickness and depth of the strata within the study area. This provided a geophysical basis for the geological division of the region. The resulting profiles from the geophysical exploration effectively reflect the basic stratigraphic conditions of the area, and the interpretations of the profiles are summarized as follows:

In the WT5 profile, the shallow section ranging from 0 to approximately −50 m primarily consists of Quaternary strata, with resistivity values between 10 and 100 Ω·m, reflecting silty clay, fine sand, medium-to-coarse sand and gravel. In localized areas, higher resistivity values ranging from 100 to 400 Ω·m are inferred to represent basalt within the Quaternary formation.

At depths of −50 to −180 m, the resistivity values range from 10 to 50 Ω·m, which suggests the presence of fine-grained sandstone, mudstone, silty mudstone, fine sandstone, gravel and granitic coarse sandstone from the Upper Cretaceous Nenjiang Formation. Below a depth of −180 m, the resistivity gradually increases to several thousand to tens of thousands of ohmmeters, indicating the presence of granite. Potential faults were inferred from this profile, with Fault F5 located beneath point 33, Fault F3 beneath point 59 and Fault F4 beneath point 83. Refer to Figure 5 for details.

In the WT11 profile, the shallow section, ranging from 0 to approximately −50 m, primarily consists of Quaternary strata, with resistivity values between 10 and 100 Ω·m, reflecting silty clay, fine sand, medium to coarse sand and gravel. In certain localized areas, higher resistivity values between 100 and 400 Ω·m are inferred to indicate basalt within the Quaternary formation. At depths of −50 to −200 m, the resistivity values range from 10 to 50 Ω·m, suggesting the presence of fine-grained sandstone, mudstone, silty mudstone, fine sandstone, gravel and granitic coarse sandstone from the Upper Cretaceous Nenjiang Formation. Below a depth of −200 m, the resistivity gradually increases to several thousand to tens of thousands of ohmmeters, indicating the presence of granite. Refer to Figure 6 for details.

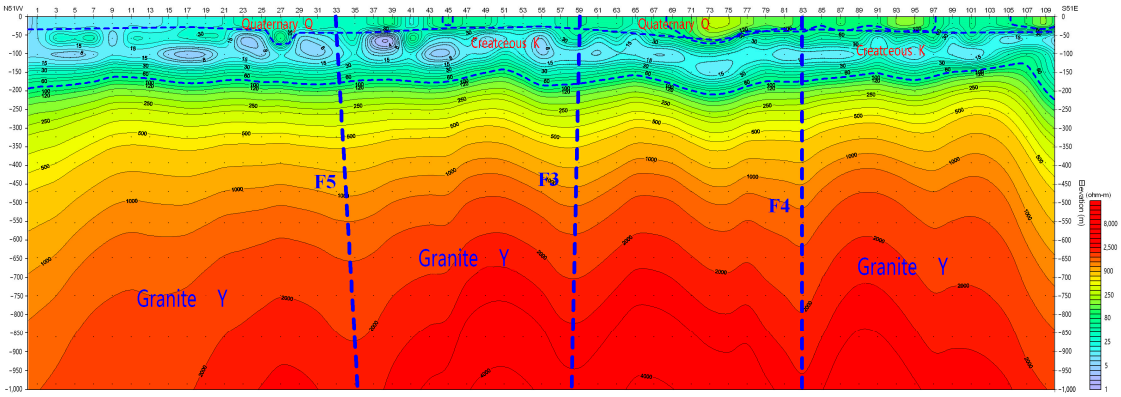


Figure 5. Controllable audio magnetotelluric method line WT05.

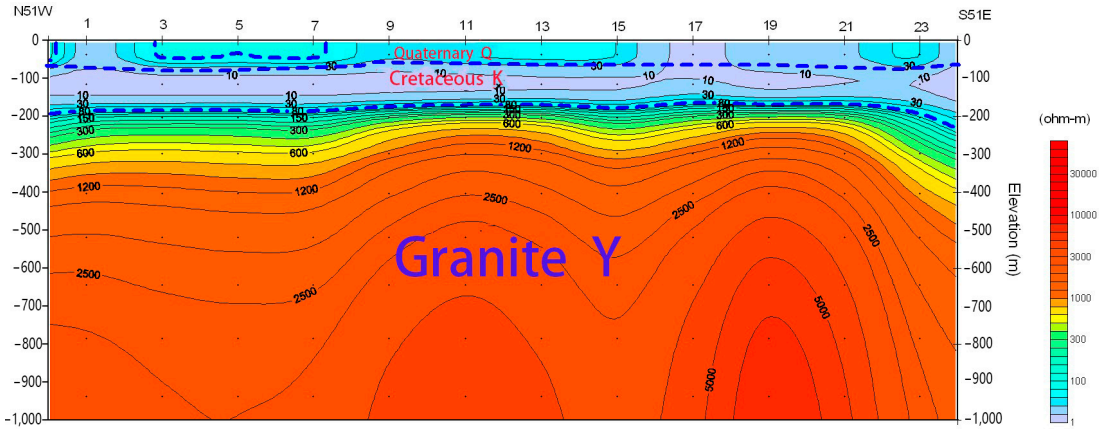


Figure 6. Controllable audio magnetotelluric method line WT11.

In the WT14 profile, the shallow section, ranging from 0 to approximately −20 m, primarily consists of Quaternary strata, with resistivity values between 10 and 100 Ω·m, reflecting silty clay, fine sand, medium to coarse sand, and gravel. At depths of −20 to −400 m, the resistivity values range from 10 to 50 Ω·m, which suggests the presence of fine-grained sandstone, mudstone, silty mudstone, fine sandstone, gravel, and granitic coarse sandstone from the Upper Cretaceous Nenjiang Formation. Below a depth of −400 m, the resistivity gradually increases to several hundred ohmmeters, indicating the presence of granite. Refer to Figure 7 for details.

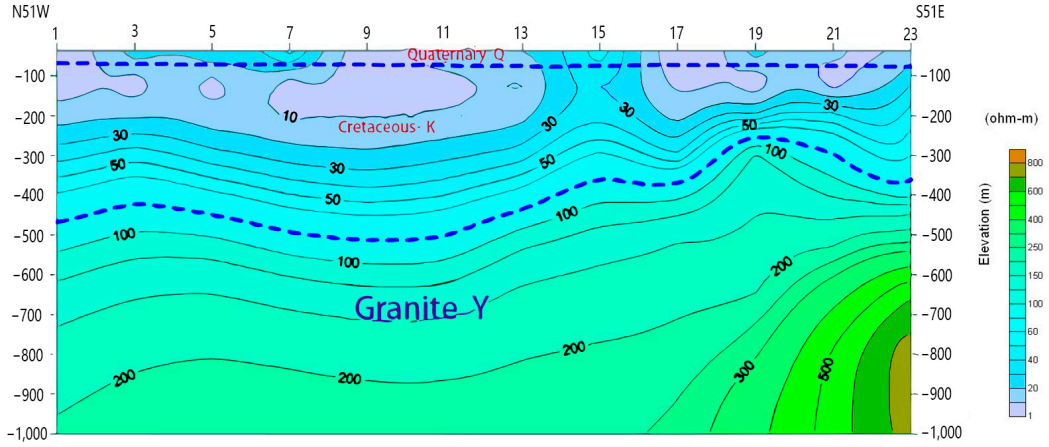


Figure 7. Controllable audio magnetotelluric method line WT14.

At the T17 profile, the shallow section, ranging from 0 to approximately −20 m, primarily consists of Quaternary strata, with resistivity values between 10 and 100 Ω·m, reflecting silty clay, fine sand, medium to coarse sand and gravel. At depths of −20 to −500 m, the resistivity values range from 10 to 50 Ω·m, suggesting the presence of fine-grained sandstone, mudstone, silty mudstone, fine sandstone, gravel and granitic coarse sandstone from the Upper Cretaceous Nenjiang Formation. Below a depth of −500 to −1000 m, the resistivity gradually increases to several hundred ohmmeters, indicating the presence of granite. Refer to Figure 8 for details.

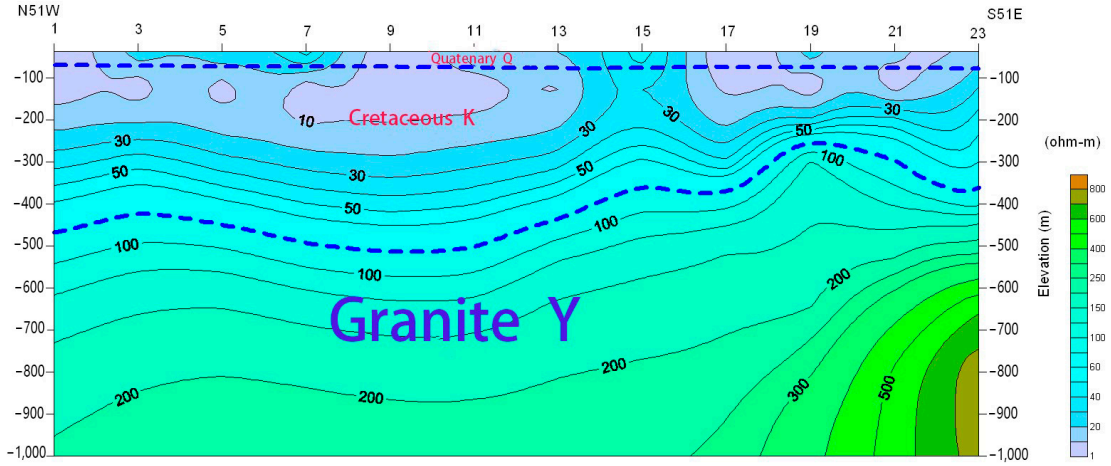


Figure 8. Controllable audio magnetotelluric method line WT17.

From the interpretation of the geophysical survey results, it is evident that the stratigraphy in this area is distinctly layered in the vertical profile, comprising a relatively high-resistivity layer in the upper section, a low-resistivity layer in the middle and a high-resistivity layer at the bottom. According to previous regional geological data, the upper relatively high-resistivity layer consists of Quaternary clay, medium-to-coarse sand layers, and basalt; the middle low-resistivity layer is characterized by Cretaceous mudstone interbedded with thin layers of fine sandstone, with the thickness gradually increasing from the northeast to the southwest; the lower high-resistivity layer is granite, with an uneven base that also deepens gradually from the northeast to the southwest.

Based on the analysis and interpretation of geophysical data, combined with geological and drilling data, it can be concluded that the thickness of the Quaternary formation in this area increases gradually from the river floodplain, to the terrace and the loess plateau, with an uneven distribution generally less than 50 m thick. Beneath the Quaternary, the underlying formation is Cretaceous, where the upper section consists of interbedded sandstone and mudstone, while the lower section comprises interbedded mudstone and fine sandstone, primarily consisting of mudstone. The thickness of the rock layers increases gradually from 80 m in the northeastern part to 300–400 m in the southwestern part of the project area. The Cretaceous area is underlain by a granite base, which overall shows a gradual increase in depth from the northeast to the southwest, with some local undulations.

4.2. Hydrogeological Survey Results

The hydrogeological survey identified a total of six mineral spring points and one soda water point. The locations and conditions of these hydrogeological investigation points are illustrated in Figure 9 below.

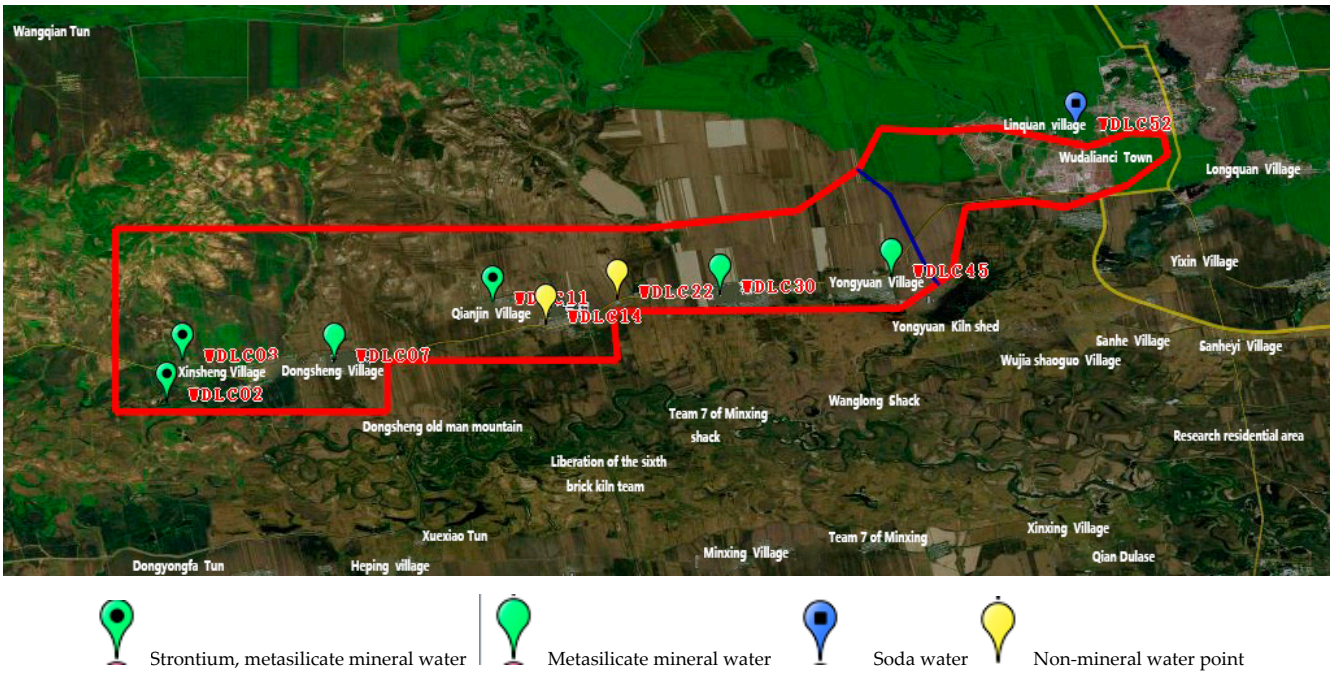


Figure 9. The locations and conditions of the hydrogeological investigation points.

Based on preliminary investigations, it can be seen that siliceous mineral water is widely distributed throughout the area, with the sole exception being the junction between the basalt plateau and the high plains, where the standards for siliceous mineral water are not met. The concentration of silicate in the survey wells is detailed in Table 2.

Table 2. Water quality of Minjing survey points.

Survey Point Number	Survey Point Location	Mineral Water Type	Silica Content (mg/L)	Strontium Content (mg/L)	Depth of Well (m)	Aquifer
WDLC02	Yongsheng Village, Tuanjie Town	Strontium, Siliceous Mineral Water	30.48	1.363	8–10	Quaternary Gravel Layer
WDLC03	Yongsheng Village	Strontium, Siliceous Mineral Water	54.58	0.564	120	Quaternary Gravel Layer, Cretaceous Sandstone
WDLC07	Dongsheng Village	Siliceous Mineral Water	48.82	0.171	30–35	Quaternary Gravel Layer, Cretaceous Sandstone
WDLC11	Qianjin Village	Strontium, Siliceous Mineral Water	34.60	0.488	33	Quaternary Sand
WDLC30	Tuanjie Town	Siliceous Mineral Water	50.09	0.104	30	Quaternary Basalt
WDLC45	Yongyuan Village	Siliceous Mineral Water	48.59	0.057	20	Quaternary Basalt
WDLC52	Linquan Village	Soda Water	Bicarbonate 263.78 (88.95%)	Sodium 96.96 (90.09%)	150	Cretaceous Sandstone and Weathered Bedrock Fractures

No bicarbonate–carbonate mineral water was found during the preliminary investigations; however, a notable concentration of bicarbonate was detected at a centralized water supply well in Linquan Village, located near Yaquan Mountain in the western part of the

project area (survey point number WDLC52), reaching a level of 263.78 mg/L. This finding provides critical information for the assessment of water resources in the area, as well as a foundation for further water quality research and development.

4.3. Analysis of Groundwater Dynamic Monitoring Results

4.3.1. Dynamic Characteristics of Siliceous Mineral Water

Based on the hydrogeological survey results, it is observed that monitoring wells QZK1 and QZK2 are located within the siliceous mineral water zone associated with the fractures and cavities of the Quaternary basalt. In contrast, monitoring wells QZK3 and QZK4 are situated in the siliceous mineral water area found within the porous loose rock formations of the Quaternary as shown in Figure 10.

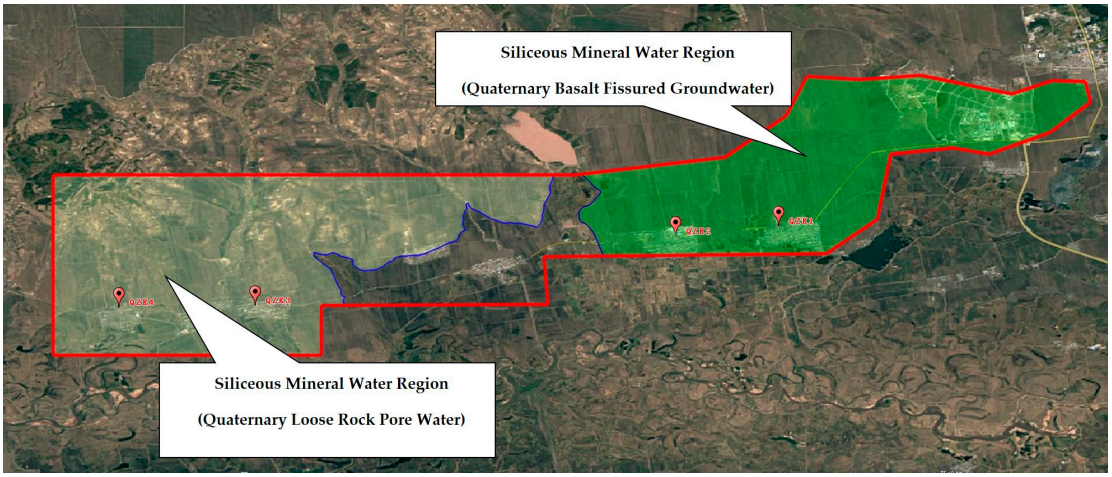


Figure 10. Schematic map of siliceous mineral water distribution area.

This differentiation indicates that the distribution and dynamics of siliceous mineral water are influenced by the lithological characteristics of the surrounding geological formations, which play a significant role in water accumulation and movement.

The monitored aquifer levels primarily consist of Quaternary aquifers and Upper Cretaceous aquifers. Monitoring has revealed significant annual variations in the groundwater levels of the siliceous mineral water exploration wells, with fluctuations ranging from 0.41 to 2.27 m. The results of the groundwater dynamic monitoring are summarized in Table 3. Based on the monitoring data, dynamic monitoring curves have been plotted, as illustrated in Figures 11–13.

Table 3. Dynamic monitoring of water levels in siliceous mineral water exploration wells.

Monitoring Hole Number	QZK1	QZK2	QZK3	QZK4
Monitoring Period	30 September 2021–30 October 2022			
Ground Elevation (m)	267.518	262.554	262.8216	248.214
Maximum Water Level Elevation (m)	252.238	252.864	260.486	240.867
Time	30 August 2022	30 August 2022	30 August 2022	10 September 2022
Minimum Water Level Elevation (m)	250.938	250.594	260.076	239.847
Time	10 March 2022	10 March 2022	20 February 2022	10 April 2022
Annual Water Level Variation (m)	1.300	2.270	0.410	1.020

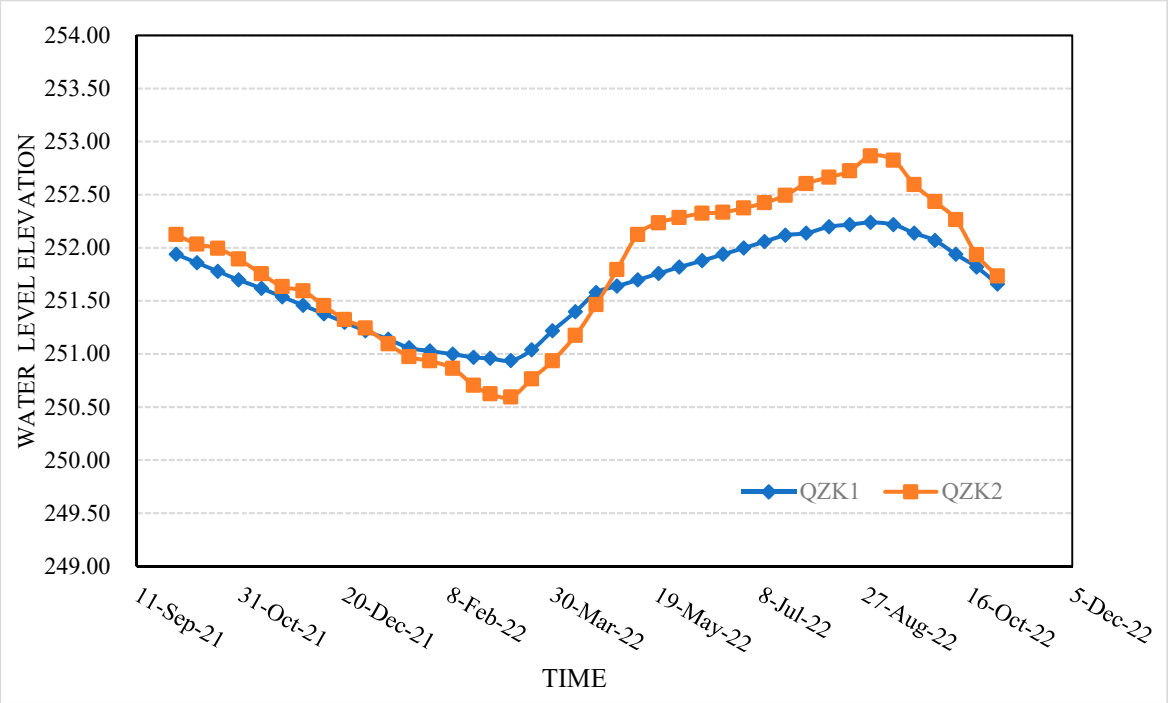


Figure 11. Dynamic observation curve of well water level (phreatic water/micro confined water).

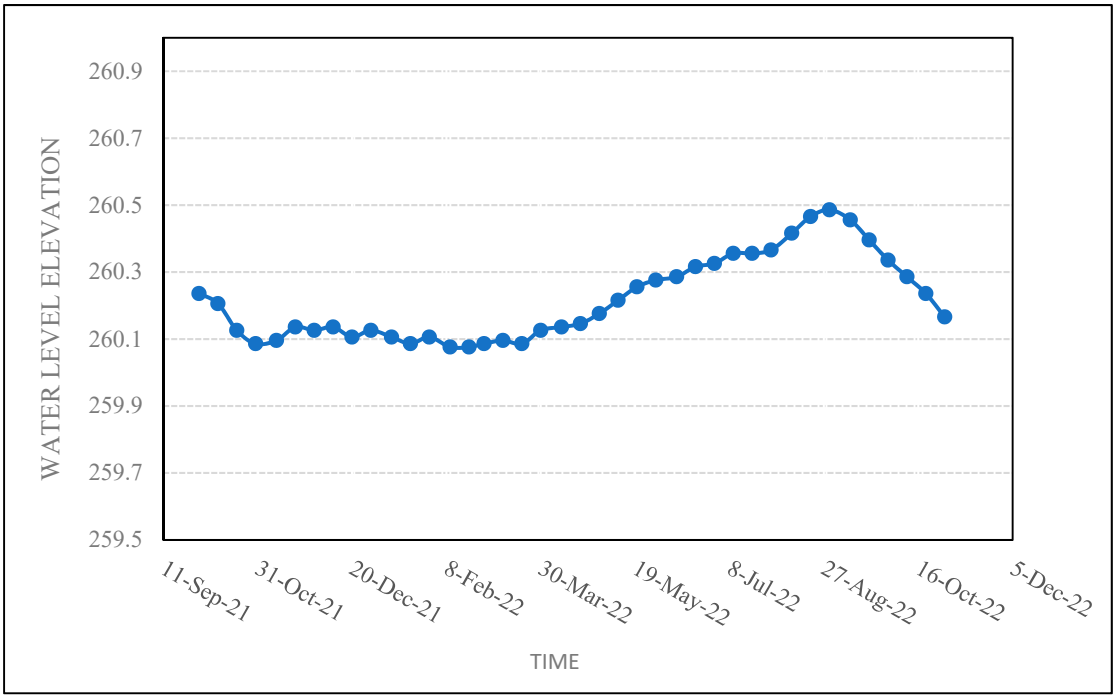


Figure 12. Dynamic observation curve of water level for well QZK3 (confined water).

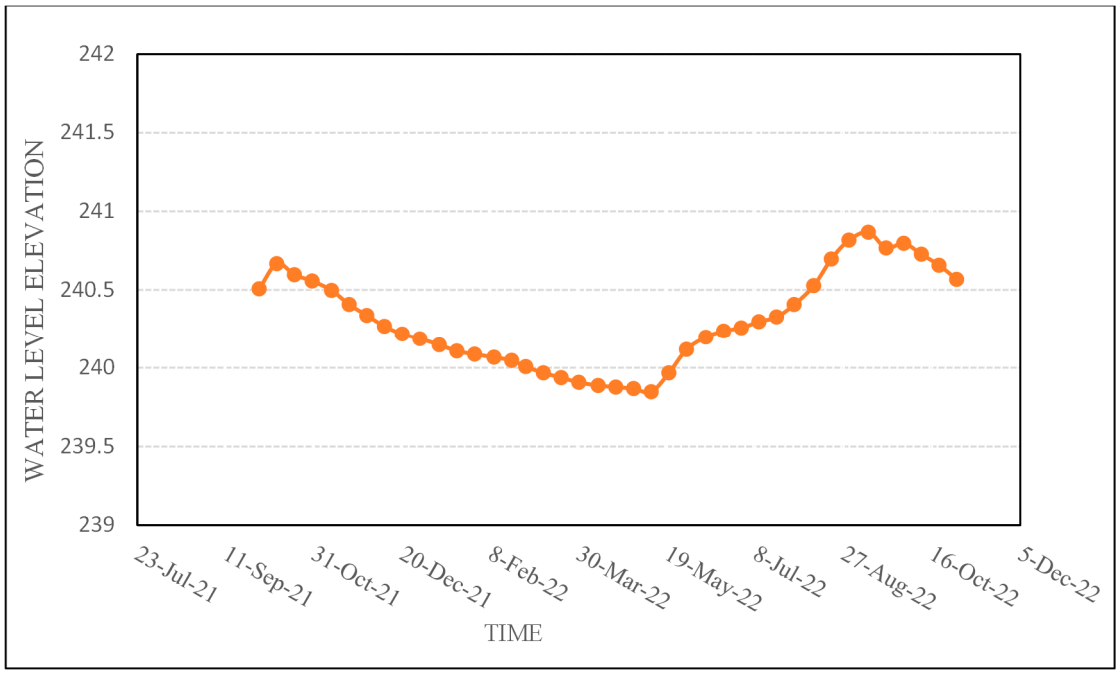


Figure 13. Dynamic observation curve of water level for well QZK4 (confined water).

From the curve graphs, it can be observed that the levels of siliceous mineral water are significantly influenced by wet and dry seasons, increasing with the amount of precipitation. Starting from the end of March each year, as the rainy season begins, the water levels gradually rise, reaching their peak by late July to early August, before gradually declining thereafter.

The water level variation patterns in these four wells indicate that the changes in QZK1 and QZK2 exhibit consistency with rainfall, responding rapidly to precipitation, which aligns with the characteristics of unconfined aquifers. In contrast, the water level variations in QZK3 and QZK4 show consistency with rainfall but respond with a slight lag, reflecting the characteristics of confined aquifers.

4.3.2. Dynamic Characteristics of Natural Soda Water

Based on the hydrogeological survey results, it is evident that monitoring wells SZK1, SZK2 and SZK3 are located within the distribution area of natural soda water shown in Figure 14.

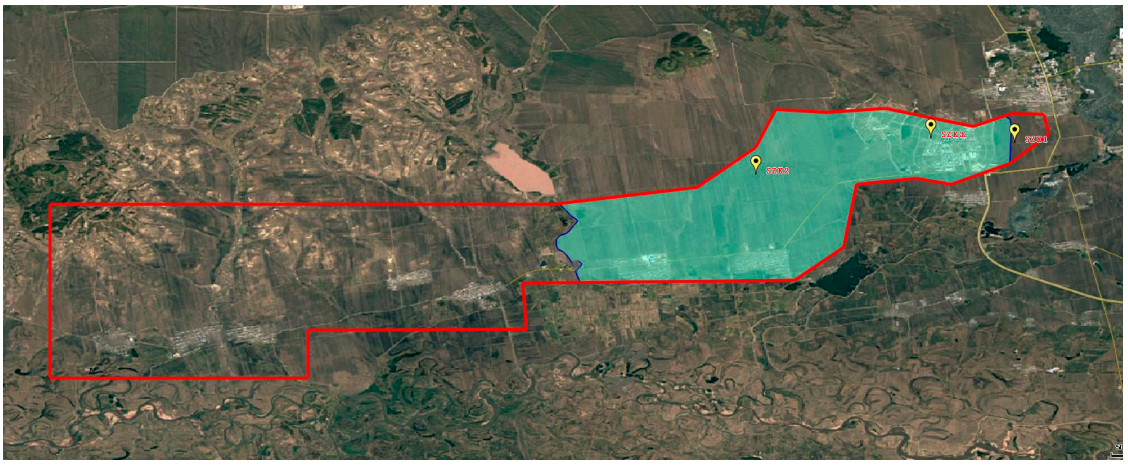


Figure 14. Schematic map of soda water distribution area.

Through dynamic monitoring of the Lower Cretaceous aquifer over one hydrological year, it was found that the annual fluctuation in groundwater levels in the Lower Cretaceous aquifer ranged from 0.12 to 0.21 m, indicating relatively small changes in the water levels. The results of the groundwater dynamic monitoring are summarized in Table 4. Dynamic monitoring curves based on actual monitoring data are presented in Figures 15–17.

Table 4. Dynamic monitoring of water level of exploration wells for natural soda water.

Monitoring Hole Number		SZK1	SZK2	SZK3
Monitoring start and end time		From 30 September 2021 to 30 October 2022.	From 10 April 2022 to 10 April 2023.	From 20 August 2022 to 30 July 2023.
Ground elevation (m)		273.591	284.014	284.437
Highest water level	Elevation (m)	264.731	248.864	282.577
	time	10 May 2022	20 August 2022	10 October 2022
Lowest water level	Elevation (m)	264.611	248.654	282.427
	time	10 December 2021	10 May 2022	20 February 2023
Water level fluctuation (m)		0.120	0.210	0.150

Through the monitoring of the water level in the deep exploration wells, it was found that the fluctuation in the static water level is extremely small and relatively stable. This indicates that the environment where natural soda water is located is relatively closed and is less affected by the wet and dry seasons outside, which is in line with the characteristics of deep confined water.

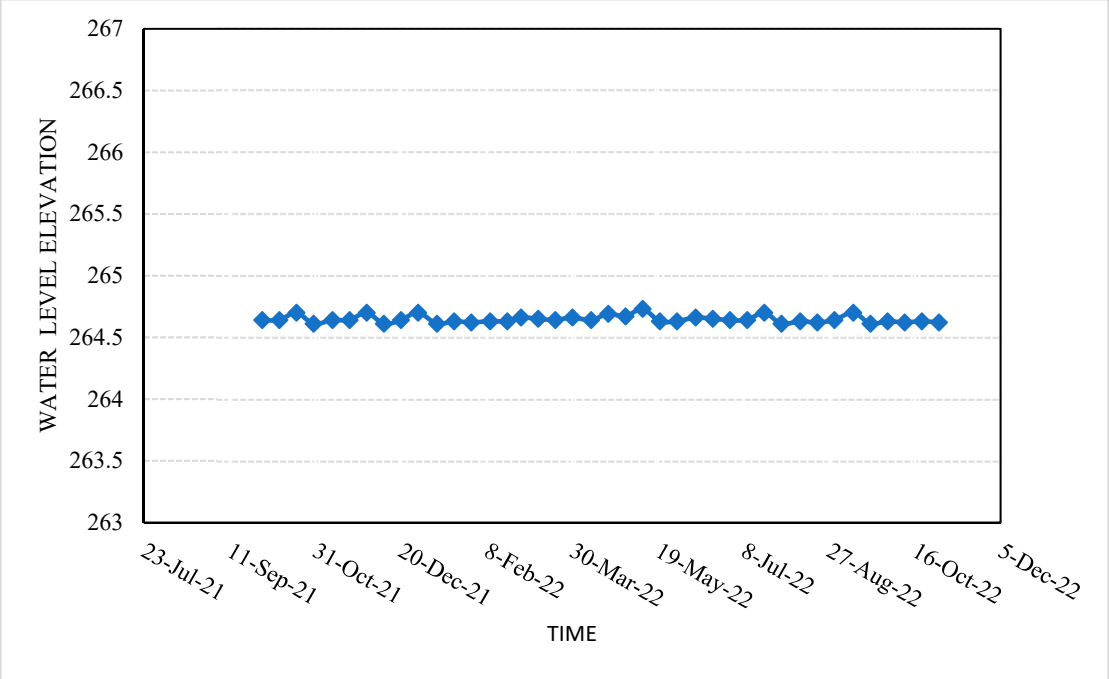


Figure 15. Dynamic observation curve of water level in well SZK1 (deep confined water—granite fracture zone).

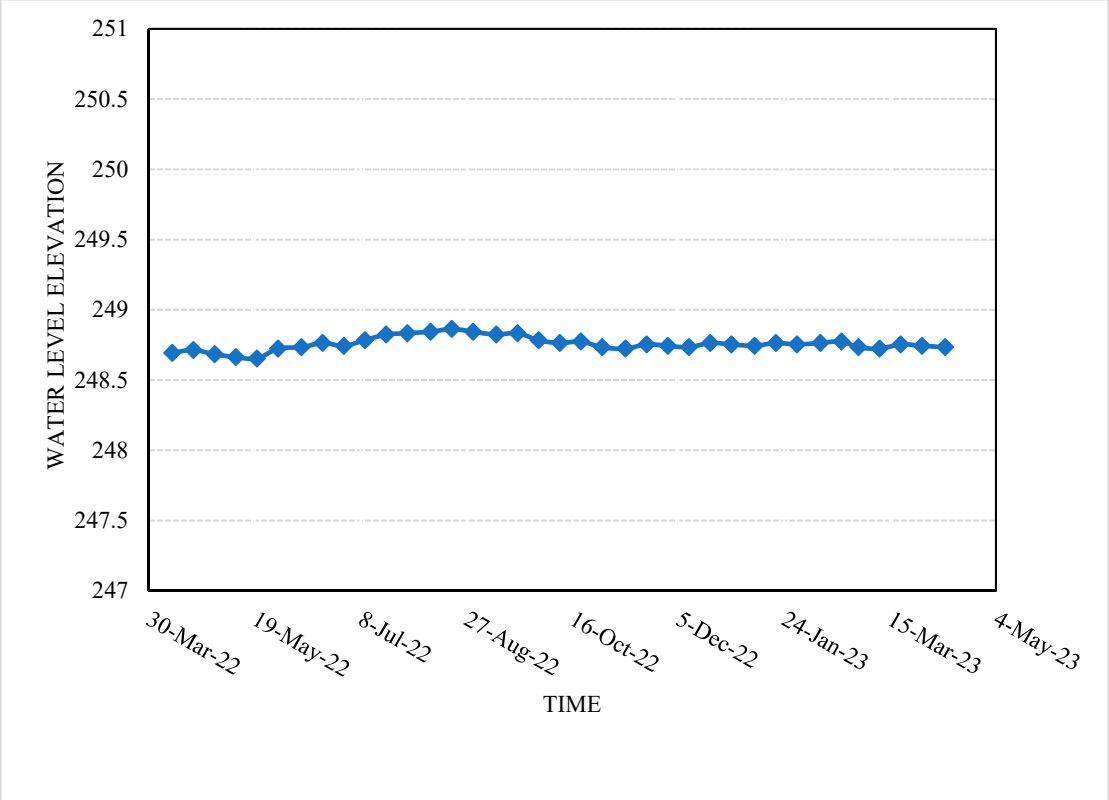


Figure 16. Dynamic observation curve of water level in well SZK2 (deep confined water).

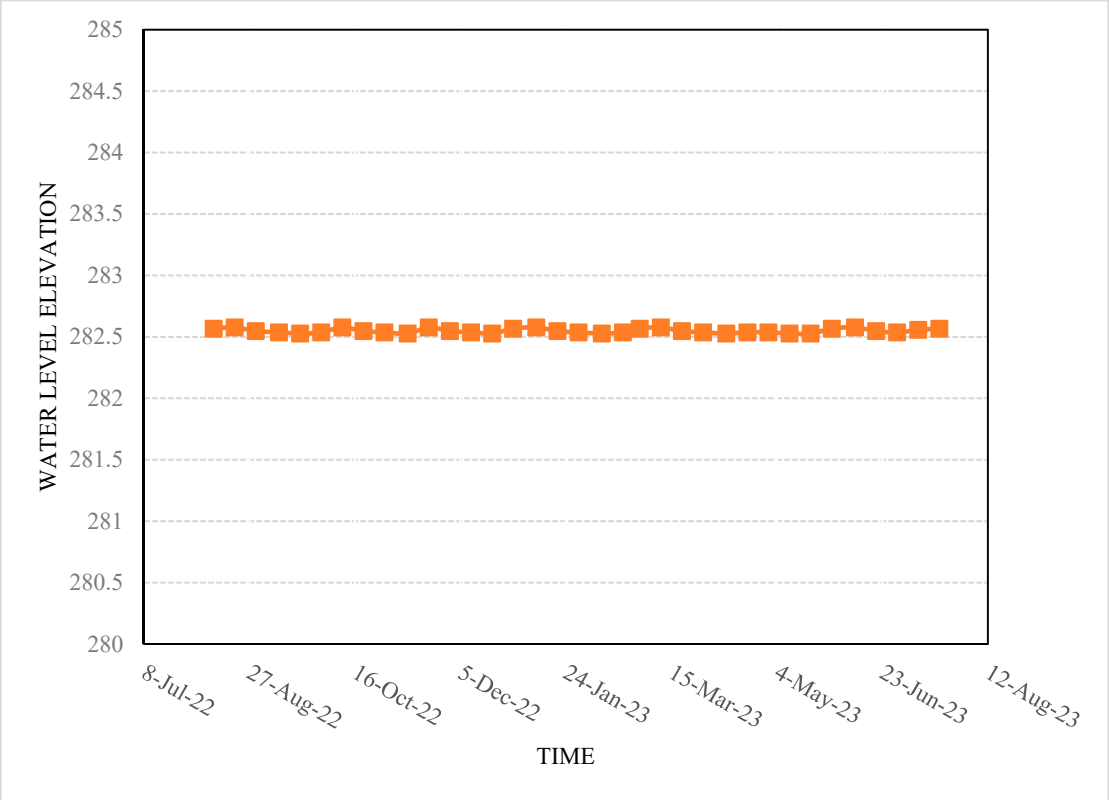


Figure 17. Dynamic observation curve of water level in well SZK3 (deep confined water).

5. Analysis of Formation Mechanism of Regional Mineral Water

5.1. Distribution Characteristics and Formation Mechanism of Siliceous Mineral Water

Siliceous mineral water exhibits a widespread distribution in the study area, predominantly concentrated along the edges of basalt plateaus and within the overlying aquifers. This water not only has abundant reserves but also displays higher concentrations of siliceous components in the groundwater from Quaternary basalt as compared to other aquifer formations. This indicates that siliceous mineral water is primarily hosted in the fissured aquifers of Quaternary basalt, with other aquifers largely relying on recharge from this layer for silicon sources. A statistical analysis of water quality data shows that while Quaternary loose rock aquifers and underlying Cretaceous sandstone also contain siliceous mineral water, the concentration of siliceous components is significantly lower than in basalt.

The formation mechanism of siliceous mineral water is complex and is influenced by geological structures, rock weathering processes and hydro-geochemical reactions. Geological structures dictate the spatial distribution, geological characteristics and hydrological conditions of the basalt layers, while the minerals within the rocks serve as the primary source of silica. Under hydro-geochemical effects, rock weathering promotes the release of silica, facilitating its transfer into the aqueous medium. Interactions between minerals such as plagioclase, pyroxene, and olivine with CO_2 and water result in the formation of clay minerals like montmorillonite and kaolinite, releasing soluble SiO_2 in the process. This mechanism is the dominant process in the formation of siliceous mineral water, highlighting how silica is concentrated under relatively closed hydrological conditions.

5.2. Distribution Characteristics and Formation Mechanism of Natural Soda Water

Natural soda water is predominantly found in basalt plateau areas, particularly within the Cretaceous Nenjiang Formation. This water typically lies at depths of around one hundred meters, with the main aquifer composed of fine sandstone interacting with the underlying weathered granite fracture zone. Due to the impact of geological structures, the water content in the soda water aquifers in this region shows significant spatial variability, especially in areas near Medicine Spring Mountain, where water resources are more abundant.

The mechanism of formation for natural soda water is closely related to the sedimentary environment of the aquifer rock groups, their chemical constituents and the groundwater recharge methods. The sedimentary environment of the Nenjiang Formation is quite complex, being primarily characterized by fluvial and deltaic depositional systems, which create suitable water storage conditions. Over long geological periods, the recharge water interacts with rock formations rich in sodium aluminum silicates and carbonate minerals, leading to the gradual accumulation of HCO_{3^-} and Na^+ ions. Notably, the transformation of sodium feldspar into clay minerals like halloysite enhances the supply of Na^+ to the water, resulting in increased pH levels and solubility, and ultimately leading to the formation of weakly alkaline natural soda water.

5.3. Distribution Characteristics and Formation Mechanism of Bicarbonate–Carbonate Mineral Water

Bicarbonate–carbonate mineral water is identified in four known water zones within the Wudalianchi area, including Medicine Spring Mountain, East Jiaodebu Mountain, Weishan Mountain, and Huoshaoshan. These zones are primarily located at the peripheries of structural uplifts or depressions, with their layout being directly influenced by geological structures. Through the continual action of secondary fault zones, CO_2 gas accumulates underground, while the overlying Cretaceous mudstone prevents gas escape. Consequently, although gas may rapidly escape when the mudstone is breached, the confined geological environment results in a limited storage capacity for CO_2.

The formation of bicarbonate–carbonate mineral water is profoundly influenced by volcanic activities and geological structures. When volcanic activities release substantial

amounts of CO_2, this gas interacts with groundwater, facilitating the formation of mineral water. The compressive and torsional fractures exhibit good sealing properties, allowing both gas and mineral water to be preserved within specific areas. Furthermore, the high pressure of the rock water enables it to penetrate through the cap layer's fissures into the overlying Cretaceous aquifer, potentially forming secondary mineral water layers. Therefore, the confinement and suitability of the tectonic environment are key conditions for the formation of bicarbonate–carbonate mineral water.

6. Conclusions

The mineral water resources in the southern area of Yaoquanshan in Wudalianchi are abundant. Affected by its unique stratum conditions and geological structure, various types of mineral water are formed. The specific conclusions of this study can be divided into the following three points:

(1) The mineral water resources in this area mainly include metasilicic acid mineral water, natural soda water and bicarbonate–carbonate mineral water. Metasilicic acid mineral water is mainly formed in the pore-fissure aquifer of Quaternary basalt and is interrelated with the Cretaceous sandstone aquifer below. Natural soda water is formed through the leaching effect between recharge water and water-bearing media in the semi-closed alkaline reducing environment of the Cretaceous area, and is mainly stored in the lower sandstone aquifer. The bicarbonate–carbonate mineral water is a special water body formed by a large amount of carbon dioxide (CO_2) released by volcanic activities entering the water to form gas and dissolved minerals.

(2) The formation mechanism of various types of mineral water depends on specific geological environments. The formation of metasilicic acid mineral water is related to the pore structure of basalt and the permeability of the underlying sandstone. The formation of natural soda water is the result of a chemical leaching process, combining the chemical composition of water with the characteristics of the strata. The bicarbonate–carbonate mineral water can be regarded as the product of volcanic activities and geological sealing conditions. Volcanic activities not only release a large amount of CO_2, but also rely on the upper mud stone cap rock to form an effective hydrogeological sealing environment to prevent the loss of gas and mineral water.

(3) The necessary condition for the formation of bicarbonate-carbonate mineral water is the closure of hydrogeological conditions. Only in a relatively closed geological structure can the loss of carbon dioxide and mineral water be effectively prevented, leading to the accumulation and enrichment of such mineral water. The bicarbonate–carbonate mineral water area of Yaoquanshan is a typical example of this closed structure. Its hydrogeological conditions promote the formation of specific types of mineral water and provide an important guarantee for the mineral water resources in the region.

Author Contributions: Conceptualization, C.L. (Chang Li); Methodology, X.S., S.H. and X.W.; Investigation, C.L. (Chuanlei Lu), Jian Zhao, X.W. and Z.S.; Resources, X.S. and C.L. (Chuansheng Li); Data curation, B.C. and J.Z.; Writing—original draft, C.L. (Chang Li); Writing—review & editing, S.H. and B.C.; Visualization, C.L. (Chuanlei Lu); Project administration, C.L. (Chuansheng Li) and Z.S. All authors have read and agreed to the published version of the manuscript.

Funding: This research was funded by China Geological Survey, grant number DD20230470.

Data Availability Statement: The original contributions presented in the study are included in the article, further inquiries can be directed to the corresponding author/s.

Conflicts of Interest: The authors declare no conflict of interest.

References

1. Yussuf, N.M.; Hossain, I.; Wagiran, H. Natural radioactivity in drinking and mineral water in Johor Bahru (Malaysia). *Sci. Res. Essays* **2012**, *7*, 1070–1075. [CrossRef]
2. John, S.O.O.; Olukotun, S.F.; Kupi, T.G.; Mathuthu, M. Health risk assessment of heavy metals and physicochemical parameters in natural mineral bottled drinking water using ICP-MS in South Africa. *Appl. Water Sci.* **2024**, *14*, 202. [CrossRef]
3. Manoj, S.; Kartheeshwari, R.M.; Keerthan, L.; Elango, L. Effects of low mineral content in bottled drinking water on human health and evaluation of optimal requirements. *J. Food Compos. Anal.* **2024**, *128*, 106052. [CrossRef]
4. Zhan, Y.; Zhao, G.Z.; Wang, J.J.; Xiao, Q.B.; Rokityansky, I.I. Crustal electric conductivity structure for Wudalianchi volcanic cluster in the Heilongjiang province, china. *Acta Petrol. Sin.* **2006**, *22*, 1494–1502.
5. Zhang, X.; Du, D.; Wu, Y.; Ye, P.; Xu, Y. Theoretical and analytical solution on vacuum preloading consolidation of landfill sludge treated by freeze–thaw and chemical preconditioning. *Acta Geotech.* **2024**, *19*, 221–238. [CrossRef]
6. Gao, S.M.; Wen, Y.J.; Zhang, W.Q.; Zhang, D.Z.; Yang, Y.S. Microbial characteristics and eco-health implication of mineral spring water in wudalianchi, northeast China. *Ying Yong Sheng Tai Xue Bao J. Appl. Ecol.* **2019**, *30*, 2865–2874.
7. Du, M.; Lei, J.; Zhao, D.; Ai, Y.; Lu, H.; Sun, C. Wudalianchi volcanism and mantle dynamics in Northeast China: New insight from Pn and Sn tomography. *Phys. Earth Planet. Inter.* **2024**, *356*, 107260. [CrossRef]
8. Zou, J.; Yang, Y.; Jia, S.; Gao, C.; Song, Z. The sources and biogeochemical cycling of carbon in the Wudalianchi UNESCO geopark volcanic system in northeast China. *Environ. Sci. Pollut. Res.* **2019**, *26*, 2918–2928. [CrossRef]
9. Di, Y.; Tian, W.; Chen, M.; Li, Z.; Liang, J. A method to estimate the pre-eruptive water content of basalts: Application to the Wudalianchi–Erkeshan–Keluo volcanic field, northeastern China. *Am. Mineral.* **2020**, *105*, 149–161. [CrossRef]
10. Jianguo, D.U.; Shengqiang, L.I.; Yi, Z.; Jinzhang, R.; Rubo, S.; Heshun, D. Geochemical characteristics of gases from the Wudalianchi volcanic area, northeastern China. *Acta Geol. Sin. Engl. Ed.* **1999**, *73*, 225–229. [CrossRef]
11. Zou, J.; Yang, Y.; Zhang, H. Sr isotope fingerprinting of multiple water-source characterizations and its environmental implications in a complex lake-groundwater system, wudalianchi, northeast China. *Chemosphere* **2018**, *212*, 1095–1103. [CrossRef] [PubMed]
12. Xie, Z.H.; Wang, J.H.; Liu, Y.; Yang, C. Health risk assessment for heavy metals in natural cold-bicarbonated mineral water, Wudalianchi. *Int. J. Chem. Eng. Appl.* **2013**, *4*, 50–53. [CrossRef]
13. Zuo, T.; Li, X.; Wang, J. Insights into natural tuff as a building material: Effects of natural joints on fracture fractal characteristics and energy evolution of rocks under impact load. *Eng. Fail. Anal.* **2024**, *163*, 108584. [CrossRef]
14. Li, N.; Fan, Q.; Sun, Q.; Sun, R. Lithogeochemistry of volcanic rocks and hosted melt inclusions in Wudalianchi, Heilongjiang, China. *J. Earth Sci.* **2009**, *20*, 771–783. [CrossRef]
15. Zhang, X.; Ye, P.; Wu, Y.; Zhai, E. Experimental study on simultaneous heat-water-salt migration of bare soil subjected to evaporation. *J. Hydrol.* **2022**, *609*, 127710. [CrossRef]
16. Zeng, Y.; Yang, C.; Wang, X.; Fang, Z.; Wu, J. Prediction of WATER Quality of Bicarbonate Mineral Water In WUDALIANCHI Based on BP Neural Network Model. *Int. Conf. Adv. Energy Environ. Res.* **2018**, *53*, 04017.
17. Zhang, H.; Yang, Y.; Zou, J.; Wen, Y.; Gao, C. The sources and dispersal of nitrate in multiple waters, constrained by multiple isotopes, in the Wudalianchi region, northeast China. *Environ. Sci. Pollut. Res. Int.* **2018**, *25*, 24348–24361. [CrossRef]
18. Van der Aa, M. Classification of mineral water types and comparison with drinking water standards. *Environ. Geol.* **2003**, *44*, 554–563. [CrossRef]
19. Petraccia, L.; Liberati, G.; Masciullo, S.G.; Grassi, M.; Fraioli, A. Water, mineral waters and health. *Clin. Nutr.* **2006**, *25*, 377–385. [CrossRef]
20. Altunışık, A. Microplastic pollution and human risk assessment in Turkish bottled natural and mineral waters. *Environ. Sci. Pollut. Res.* **2023**, *30*, 39815–39825. [CrossRef]
21. Huang, X.; Wang, S.; Wang, H.; Wang, S.; Qi, S. Hidden magma reservoirs: Insights from helium and carbon isotopic compositions in shallow groundwater beneath the Wudalianchi volcanic field, Northeastern China. *Chem. Geol.* **2024**, *666*, 122310. [CrossRef]
22. Huang, Q.; Yang, F.; Cao, H.; Cheng, J.; Jiang, M.; Li, M.; Ni, H.; Xie, L. Comparison of microbial diversity of two typical volcanic soils in Wudalianchi, China. *Microorganisms* **2024**, *12*, 656. [CrossRef] [PubMed]
23. Sunardi, D.; Chandra, D.N.; Medise, B.E.; Manikam, N.R.M.; Friska, D.; Lestari, W.; Insani, P.N.C. Health effects of alkaline, oxygenated, and demineralized water compared to mineral water among healthy population: A systematic review. *Rev. Environ. Health* **2024**, *39*, 339–349. [CrossRef] [PubMed]
24. Liu, J.; Ai, Y.; Chen, Y.; Lei, J. The crust-mantle velocity structure beneath the Wudalianchi-Erkeshan-Keluo volcanic belt by joint inversion of receiver functions and ambient noise. *Phys. Earth Planet. Inter.* **2024**, *351*, 107194. [CrossRef]
25. Zhang, Y.; Zhang, X. Research on the Development Model of Cultural and Creative Industry of Tourism in Wudalianchi Scenic Area in Heilongjiang Province. In Proceedings of the 2020 International Conference on Management, Economy and Law (ICMEL 2020), Hangzhou, China, 6–8 March 2020; Atlantis Press: Amsterdam, The Netherlands, 2020; pp. 199–204.

Disclaimer/Publisher's Note: The statements, opinions and data contained in all publications are solely those of the individual author(s) and contributor(s) and not of MDPI and/or the editor(s). MDPI and/or the editor(s) disclaim responsibility for any injury to people or property resulting from any ideas, methods, instructions or products referred to in the content.